High concentration heavy metal removal by indigenous ureolytic bacteria: a comparative study with Sporosarcina pasteurii for Zn and Cd bioprecipitation

Physics and Chemistry of the Earth 143 (2026) 104347

Contents lists available at ScienceDirect

Physics and Chemistry of the Earth

journal homepage: www.elsevier.com/locate/pce

High concentration heavy metal removal by indigenous ureolytic bacteria: A comparative study with *Sporosarcina pasteurii* for Zn and Cd bioprecipitation

Ugochukwu Oliver Ukachi [a], Armstrong Ighodalo Omoregie [b], Hazlami Fikri Basri [c], Charles K.S. Moy [d], Adharsh Rajasekar [a,e,*]

[a] Jiangsu Key Laboratory of Atmospheric Environment Monitoring and Pollution Control (AEMPC), Collaborative Innovation Center of Atmospheric Environment and Equipment Technology (CIC-AEET), Nanjing University of Information Science &Technology, Nanjing, 210044, China
[b] Research Centre for Borneo Regionalism and Conservation, School of Built Environment, University of Technology Sarawak, No. 1 Jalan Universiti, Sibu, 96000, Sarawak, Malaysia
[c] Department of Water and Environmental Engineering, Faculty of Civil Engineering, Universiti Teknologi Malaysia, 81310, Skudai, Johor, Malaysia
[d] Department of Civil Engineering, Xi'an Jiaotong-Liverpool University, Suzhou, Jiangsu, 215123, China
[e] School of Geography and Environmental Science, University of Reading, Reading, RG67BE, United Kingdom

ARTICLE INFO

Keywords:
Ureolysis
Carbonate precipitation
Biostimulation
Metal immobilization
Biogenic minerals

ABSTRACT

Heavy metal pollution from industrial activities threatens aquatic ecosystems and human health. While microbially induced carbonate precipitation (MICP) offers a promising bioremediation strategy, most studies rely on laboratory-adapted strains, such as *Sporosarcina pasteurii*, and provide limited comparisons with indigenous microbes under identical stress conditions. We hypothesized that an indigenous ureolytic bacterium, pre-adapted to metal-contaminated environments, would outperform *S. pasteurii* under suboptimal temperatures and high cadmium (Cd) and zinc (Zn) concentrations, a gap unaddressed in prior MICP literature. Here, we compare the carbonate precipitation efficiency of *Comamonas sp. HMZC* (B11), isolated from a polluted river catchment, with *S. pasteurii* at 15 °C and 30 °C using 6 mM and 8 mM Cd or Zn over 96 h. Strain B11 achieved >90% removal of both metals at 30 °C, comparable to or slightly better than *S. pasteuri*, and maintained 70–85% efficiency at 15 °C, with a statistically significant advantage in Zn removal under cold stress. SEM-EDS and XRD confirmed well-crystallized $CdCO_3$ and $ZnCO_3$ precipitates, with B11 yielding higher crystallinity. These results support the use of indigenous strains, such as B11, for biostimulation-based, site-specific remediation of heavy-metal-contaminated waters.

1. Introduction

Heavy metal pollution is a critical environmental issue, with zinc (Zn) and cadmium (Cd) among the most pervasive contaminants. Both metals originate primarily from metallurgical processing, and industrial emissions, with cadmium often occurring as a by-product of zinc extraction. (Das et al., 2023; Jin et al., 2025). Although zinc is an essential micronutrient, excessive accumulation can disrupt aquatic ecosystems and soil microbial balance. In contrast, cadmium is a non-essential and highly toxic metal, classified as a human carcinogen, with significant risks of bioaccumulation and trophic transfer (Mitra et al., 2022; Y. Zeng et al., 2021). A recent global inventory estimated cadmium reserves at roughly 3.3 million tonnes, much of it located near populated or ecologically sensitive regions, emphasizing its long-term contamination potential (Werner et al., 2024). Besides, prolonged exposure to cadmium, for instance, has been linked to renal dysfunction, skeletal damage, and respiratory disorders, while zinc, although an essential trace element, can be toxic at high levels, causing gastrointestinal distress and disrupting nutrient absorption (Liu et al., 2025). The urgency of mitigating such impacts has led to extensive research on efficient and sustainable remediation methods.

Conventional approaches to heavy metal remediation, including chemical precipitation, ion exchange, and electrochemical treatments, have demonstrated varying degrees of success (Qin et al., 2019).

* Corresponding author. Jiangsu Key Laboratory of Atmospheric Environment Monitoring and Pollution Control (AEMPC), Collaborative Innovation Center of Atmospheric Environment and Equipment Technology (CIC-AEET), Nanjing University of Information Science &Technology, Nanjing, 210044, China.
E-mail address: a.rajasekar@reading.ac.uk (A. Rajasekar).

https://doi.org/10.1016/j.pce.2026.104347
Received 24 October 2025; Received in revised form 8 February 2026; Accepted 12 February 2026
Available online 14 February 2026

However, these techniques often suffer from high operational costs, the production of secondary pollutants, and limited efficacy in large-scale applications (L. Wang et al., 2017; W. Wu et al., 2022; C. Zeng et al., 2020). This has spurred the search for environmentally friendly and cost-effective alternatives, with bioremediation emerging as one of the most promising strategies. Microbially induced carbonate precipitation (MICP) is an innovative bioremediation technique that exploits the metabolic capabilities of ureolytic bacteria to convert soluble heavy metals into stable, insoluble carbonate forms; this method has garnered considerable attention due to its potential for heavy metal immobilization in contaminated soils and water bodies (A. Kumar et al., 2023; Shan et al., 2021).

The mechanism behind MICP involves urease-producing bacteria that hydrolyze urea into ammonia and carbonate ions. These ions then react with metal cations in the environment, leading to the precipitation of metal carbonates (Y. Kim et al., 2021; Rajasekar et al., 2021). Among the bacteria studied for this purpose, *Sporosarcina pasteurii* has become a model organism due to its robust urease activity and demonstrated ability to precipitate a variety of heavy metals, including Zn and Cd. Several studies have reported the successful application of *S. pasteurii* in immobilizing toxic metals, with researchers observing significant reductions in metal bioavailability following treatment (Ashraf et al., 2017; Castro-Alonso et al., 2019; A. Kumar et al., 2023). However, most of this research has focused on laboratory strains of bacteria, which may not fully reflect the diversity and adaptability of microbial communities in contaminated sites (Fux et al., 2005).

Bioremediation strategies generally consist of two main approaches: biostimulation and bioaugmentation. Biostimulation involves enhancing natural biodegradation processes by optimizing environmental conditions (such as nutrient amendment, pH adjustment, oxygen supply) to stimulate the activity and growth of indigenous microbial populations already present at a contaminated site (Omokhagbor Adams et al., 2020; Singh and Christina, 2022; Tyagi et al., 2011). This method is often favored due to its reliance on microorganisms naturally adapted to the local environment, potentially leading to more stable, sustainable, and cost-effective remediation outcomes (B. L. Kumar and Gopal, 2015; Omokhagbor Adams et al., 2020; Singh and Christina, 2022). Conversely, bioaugmentation entails the introduction of exogenous (non-indigenous) microorganisms, typically laboratory-cultured strains with specific catabolic capabilities, into a contaminated area to accelerate pollutant degradation (Inamuddin et al., 2022; Tyagi et al., 2011). While bioaugmentation can offer targeted and potentially rapid contaminant removal under controlled conditions, its effectiveness in complex natural environments is frequently hampered by several challenges. Introduced strains may struggle with survival, establishment, and integration into existing microbial communities due to competition with native flora, predation, and an inability to tolerate site-specific stressors such as extreme pH, fluctuating temperatures, or high pollutant concentrations (Inamuddin et al., 2022; Kuppan et al., 2024; Kurniawan et al., 2022; Mishra et al., 2020; Tyagi et al., 2011). Consequently, understanding and leveraging the metabolic potential of indigenous bacteria becomes paramount for developing robust and environmentally sound remediation solutions.

Indigenous bacteria, naturally present in polluted environments, represent an underexplored resource for bioremediation; these microorganisms are often adapted to local conditions, including the presence of high metal concentrations, and may possess unique metabolic pathways that enhance their bioremediation capabilities (Colin et al., 2012; Singh and Christina, 2022). Studies have shown that indigenous bacteria can tolerate and even thrive in metal-stressed environments, leading to their potential for enhanced metal precipitation and immobilization (Keshri et al., 2024); for instance, recent works have demonstrated that indigenous microbial communities in mining-impacted soils can precipitate heavy metals as efficiently as standard laboratory strains, possibly due to their long-term exposure and adaptive mechanisms (Hu et al., 2024; Abbasi et al., 2024; Oziegbe et al., 2021). Despite this, there remains a notable gap in the literature; there are very few studies that directly compare indigenous and well-established standard laboratory ureolytic bacteria strains like *Sporosarcina pasteurii* for carbonate precipitation under identical environmental conditions.

This study addresses a critical gap: how does an indigenous ureolytic strain, pre-adapted to metal stress, compare with the model organism *S. pasteurii* under identical MICP conditions involving high Cd/Zn concentrations and suboptimal temperatures?" A simplified overview of the MICP-based metal-removal process and the experimental design is provided in Fig. 1. The two core objectives were: 1. Compare precipitation efficiency between *Comamonas* sp. HMZC (B11) and *S. pasteurii* and 2. Evaluate performance under two temperatures (15 °C and 30 °C) and two metal concentrations (6 mM and 8 mM). This study adopts an integrated approach, combining biological performance metrics (urea degradation kinetics and metal removal efficiency) with mineralogical characterization (SEM-EDS and XRD) to provide a comprehensive assessment of carbonate precipitation—not only in terms of *how much* metal is removed, but also *how stably* it is immobilized. We specifically selected Cd and Zn because of their frequent co-occurrence in mining and industrial effluents, distinct toxicity profiles, and environmental persistence. The tested concentrations (6–8 mM) reflect elevated but ecologically relevant levels found near smelters and electroplating sites. By integrating biological performance (urea degradation, removal efficiency) with mineralogical characterization (SEM-EDS, XRD), this work evaluates metal removal concentration under varying temperature conditions. Ultimately, we aim to assess whether indigenous strains such as B11, through natural adaptation, provide a more resilient, sustainable alternative to bioaugmentation, thereby potentially supporting biostimulation as a possible practical strategy for field-scale remediation.

2. Materials and methods

2.1. Bacteria screening and urea degradation test

The bacteria were isolated from a polluted catchment (Qunying River) near Pukou, Nanjing, China, using the serial dilution and pour plate method. Nutrient agar (hopebio™, China) was used for initial isolation. The bacteria were further tested for urea degradation. The detailed protocol, along with the urea degradation ability, is provided in our previous paper (Rajasekar et al., 2024). *Sporosarcina Pasteurii* was bought from the Guangdong Microbial Culture Collection Centre.

2.2. Metal toxicity test

The selected bacteria were exposed to increasing concentrations of $ZnCl_2$ and $CdCl_2$ (1-10 mM) on nutrient agar. After the metal solution was added, bacterial suspensions were inoculated and incubated at 30 °C for seven days. This protocol is based on a previous study by Rajasekar et al. (2025). Colony formation on agar plates determined bacterial tolerance to heavy metal concentrations. Controls without bacteria were included for comparison.

2.3. Genomic identification of heavy metal-resistant bacteria

The most resistant bacteria were selected for genomic analysis. DNA extraction was followed by amplification using the 27F and 1492R primers (Frank et al., 2008; Muyzer et al., 1993). PCR products were purified and sequenced. BLAST analysis (Altschul et al., 1990) compared the sequences with the NCBI database. The strain accession number is OQ826684, and it was identified as *Comamonas sp.* HMZC, 99.93%, 1417 basepairs.

2.4. Heavy metal carbonate precipitation studies

The bacteria exhibiting high urease activity were tested for their ability to precipitate heavy metal carbonates. Cultures were grown in

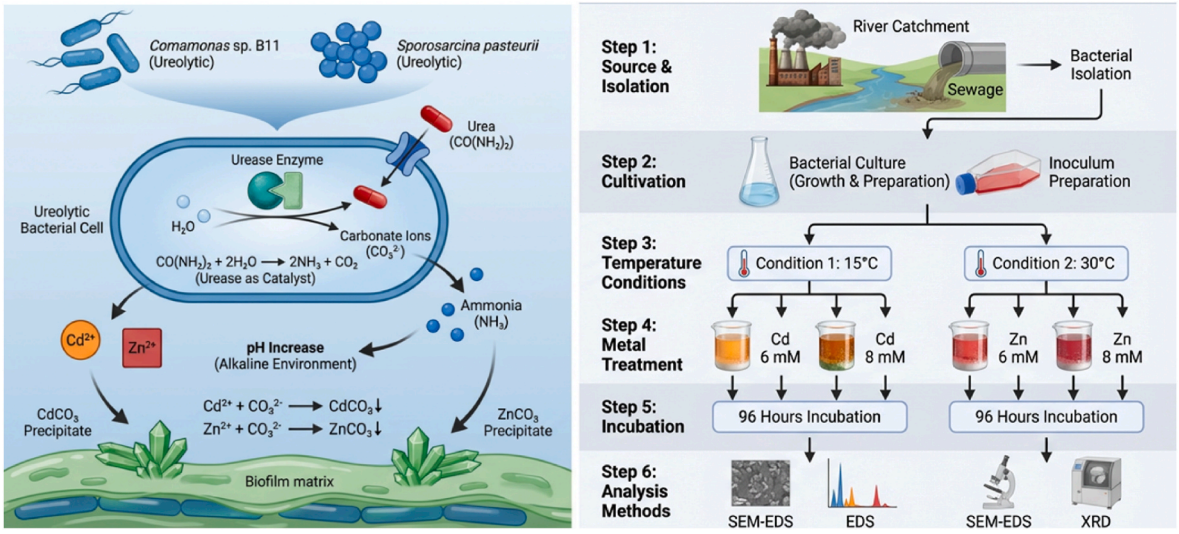

Fig. 1. Schematic of MICP-based Cd/Zn removal: (left) ureolytic bacteria convert urea into carbonate, precipitating dissolved metals as stable carbonates. (Right) The study compares the indigenous strain B11 with *S. pasteurii* under high metal loads and two temperatures (15 °C and 30 °C).

100 mL solutions containing 6 and 8 mM $ZnCl_2$ and $CdCl_2$, with 333 mM urea added as a source for carbonate precipitation. The experiment was conducted at pH 7, at 15 °C and 30 °C, and at 180 rpm for 96 h (Table 1). The heavy metal concentration and urea degradation were determined every 24 h to quantify the remaining heavy metal and urea in the solution. Urea concentration was determined using a colorimetric diacetyl monoxime method with modifications as described by Langenfeld et al. (2021). The assay was conducted in the presence of sulfuric acid, phosphoric acid, thiosemicarbazide, and ferric chloride, resulting in a pink chromophore with an absorbance measured at 520 nm. Urea concentrations were quantified from a linear calibration curve over the 0.4-5.0 mM range.

After the experiment, the precipitates were collected by filtration and dried for further analysis. The removal efficiency of metals was calculated using the initial and final concentrations in the solution. The experimental temperatures of 15 °C and 30 °C were selected to reflect environmentally relevant conditions in aquatic ecosystems, ranging from cooler temperate waters to warmer surface waters in contaminated sites, ensuring applicability to diverse field scenarios. These temperatures also align with the optimal range for urease activity in ureolytic bacteria, with 30 °C approaching the peak activity for *Sporosarcina pasteurii,* and 15 °C testing microbial performance under suboptimal conditions (Chen et al., 2022). The metal concentrations of 6 mM and 8 mM for zinc and cadmium were chosen to represent elevated contamination levels found in heavily polluted aquatic environments, such as those impacted by mining or industrial effluents (Zhou et al., 2020). These concentrations challenge microbial tolerance while remaining within the range tested in prior MICP studies, allowing for a robust comparison of precipitation efficiency between the indigenous strain *Comamonas sp.* HMZC and *S. pasteurii*. This design ensures the study's relevance to real-world bioremediation while providing insights into microbial performance under varying environmental stresses.

2.5. Quantification and characterization of precipitates

Precipitates were visualized using a Scanning Electron Microscope-Energy dispersive spectroscopy (SEM-EDS) (FEI Quanta 400FEG, Thermo Fisher Scientific). The samples were gold-coated before performing SEM-EDS. Residual heavy metal concentrations were determined using Flame Atomic Absorption Spectroscopy (ZEEnit 700P, Analytik Jena GmbH, Germany). A series of zinc and cadmium concentrations was prepared, and a standard curve was plotted to determine heavy metal concentration. Precipitates were analyzed using a Bruker D8 Advance X-ray diffractometer with Cu Kα radiation ($\lambda = 1.5406$ Å). Scans were performed from $2\theta = 5°$ to 90° with a step size of 0.02° and a scan speed of 8°/min. Phase identification was conducted using Match! Software as it incorporates the ICDD database (Kabekkodu et al., 2024).

Table 1
Summary of experimental design: bacterial strains, metal types, concentrations, temperatures, initial pH, incubation duration, and replicate number ($n = 3$).

Bacterial Strain	Metal Type	Metal Concentration (mM)	Temperature (°C)	Initial pH	Incubation Duration (h)	Replicates
Comamonas sp. HMZC (B11)	Cd	6	15	7.0	96	3
Comamonas sp. HMZC (B11)	Cd	6	30	7.0	96	3
Comamonas sp. HMZC (B11)	Cd	8	15	7.0	96	3
Comamonas sp. HMZC (B11)	Cd	8	30	7.0	96	3
Comamonas sp. HMZC (B11)	Zn	6	15	7.0	96	3
Comamonas sp. HMZC (B11)	Zn	6	30	7.0	96	3
Comamonas sp. HMZC (B11)	Zn	8	15	7.0	96	3
Comamonas sp. HMZC (B11)	Zn	8	30	7.0	96	3
Sporosarcina pasteurii	Cd	6	15	7.0	96	3
Sporosarcina pasteurii	Cd	6	30	7.0	96	3
Sporosarcina pasteurii	Cd	8	15	7.0	96	3
Sporosarcina pasteurii	Cd	8	30	7.0	96	3
Sporosarcina pasteurii	Zn	6	15	7.0	96	3
Sporosarcina pasteurii	Zn	6	30	7.0	96	3
Sporosarcina pasteurii	Zn	8	15	7.0	96	3
Sporosarcina pasteurii	Zn	8	30	7.0	96	3

2.6. Statistical analysis

All experiments were performed in triplicate, and data were analyzed using GraphPad Prism 10 and SPSS 28.0. Results are presented as means ± standard deviation. ANOVA was used to assess statistical significance, with a 95% confidence interval. We verified that the data satisfied the assumptions of normality (assessed using the Shapiro-Wilk test) and homoscedasticity (evaluated using Levene's test) before conducting the ANOVA. In addition to ANOVA, Pearson correlation analysis was performed to assess the linear relationship between % urea degraded and % metal removed across all experimental conditions (n = 64). OriginPro 24 and Graphpad Prism 10 were used to plot the bar graphs. Error bars in the figures represent standard deviations.

3. Results and discussion

3.1. Urea degradation

Urea degradation by the indigenous ureolytic bacterium *Comamonas* sp. HMZC (B11) and the model strain *Sporosarcina pasteurii* (SP) were assessed over 96 h at temperatures of 15 °C and 30 °C in the presence of cadmium (Cd) or zinc (Zn) at concentrations of 6 mM and 8 mM (Fig. 2). Across all experimental conditions, both strains demonstrated higher urea degradation rates at 30 °C compared to 15 °C, with degradation levels being approximately 20–30% lower at the cooler temperature, reflecting the influence of thermal conditions on enzymatic activity. Specifically, at 15 °C with 6 mM Cd, strain B11 exhibited significantly higher urea degradation than SP at the 24-h mark ($p = 0.017$), although no notable differences were observed in subsequent time points. In the 8 mM Cd condition at 15 °C, B11 maintained degradation rates comparable to SP following the initial 48 h. At 30 °C with 8 mM Cd, SP initially outperformed B11 at 24 and 48 h ($p < 0.001$), but B11 caught up and matched SP's performance by 72–96 h. Similarly, in the 8 mM Zn condition at 30 °C, SP showed better degradation at 72 and 96 h ($p < 0.001$). These temporal patterns highlight variations in the strains' responses to metal stress and temperature, with B11 often displaying resilience in sustaining activity over time.

3.2. Temporal dynamics of urea degradation: repeated measures ANOVA

"Repeated measures ANOVA revealed significant time-dependent differences in urea degradation between B11 and *S. pasteurii* under specific stress conditions (Table S1). For Cd (6 mM, 15 °C), B11 degraded urea significantly faster than SP at 24 h ($p < 0.05$), though differences diminished by 96 h. Under high Cd stress (8 mM, 30 °C), SP outperformed B11 at 24–48 h ($p < 0.001$), but B11 matched SP by 72–96 h. Similarly, in Zn (8 mM, 30 °C), SP maintained superior degradation until 96 h ($p < 0.001$). These temporal patterns highlight

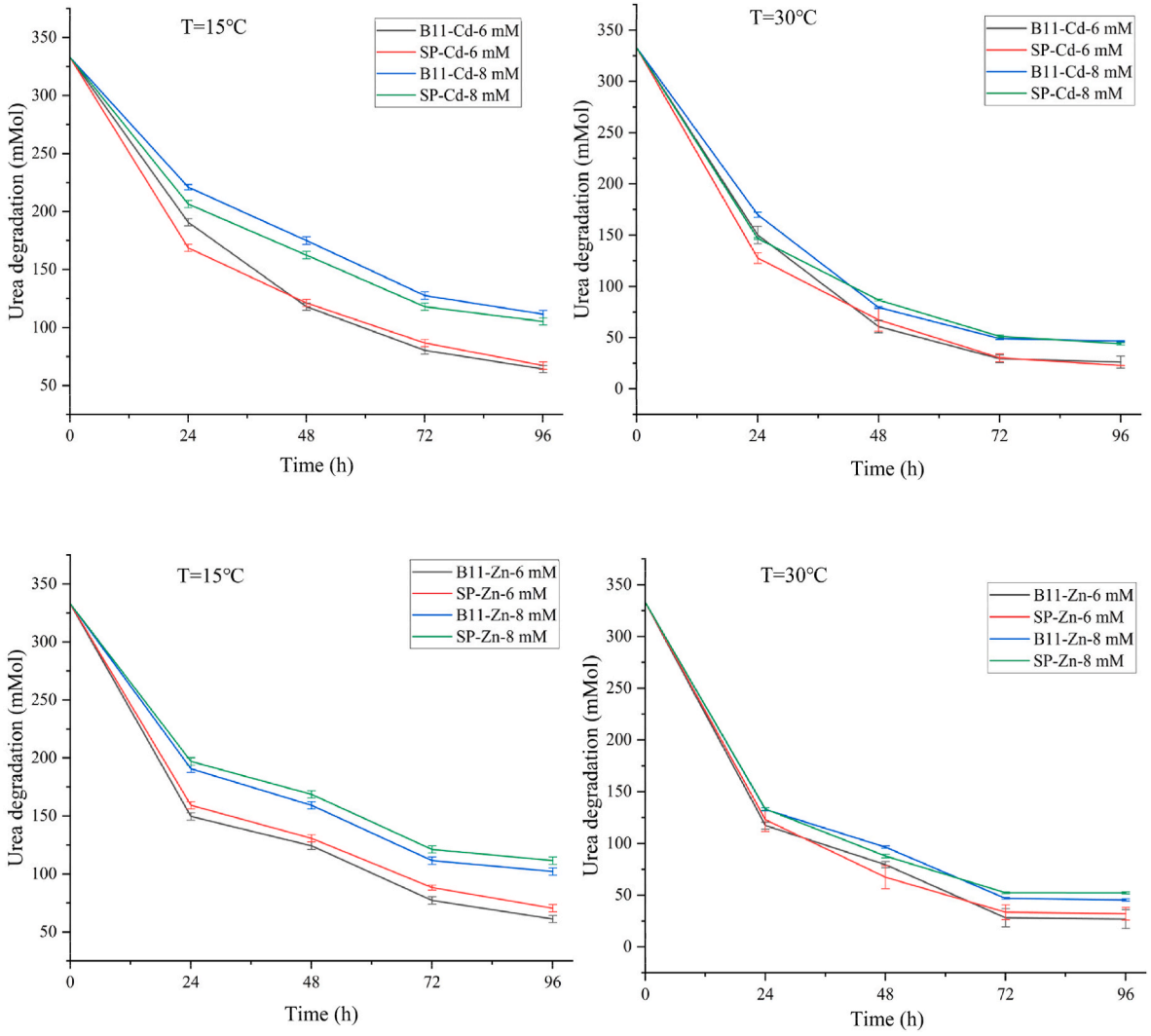

Fig. 2. Urea degradation by B11 (*Comamonas* sp. HMZC) and SP (*Sporosarcina pasteurii*) at different temperatures and heavy metal concentrations. Values represent mean ± SD ($n = 3$). Error bars represent standard deviation.

B11's resilience in sustaining long-term activity despite initial lag under metal stress.

3.3. Cadmium removal efficiency

The cadmium removal efficiency of *Sporosarcina pasteurii* (SP) and the indigenous bacterium *Comamonas* sp. HMZC (B11) was evaluated at metal concentrations of 6 mM and 8 mM under incubation temperatures of 15 °C and 30 °C over 96 h (Figs. 3 and 4). Both strains consistently achieved removal rates exceeding 94% across all tested conditions, demonstrating robust performance in cadmium precipitation via microbially induced carbonate precipitation (MICP). In the 6 mM Cd experiments, both B11 and SP reached removal efficiencies greater than 95% by the end of the 96 h, with SP exhibiting a marginally higher efficiency during the early phases at 15 °C. For the higher concentration of 8 mM Cd at 30 °C, B11 attained a removal efficiency of 96.2%, slightly surpassing SP's 94.6%. No cadmium removal was observed in the control groups lacking bacterial inoculation, confirming that the precipitation was microbiologically driven. These results indicate that temperature and metal concentration influence the kinetics of removal, with optimal performance observed at the higher temperature.

3.4. Zinc removal efficiency

Zinc removal efficiency by *Sporosarcina pasteurii* (SP) and *Comamonas* sp. HMZC (B11) was investigated at concentrations of 6 mM and 8 mM at temperatures of 15 °C and 30 °C over a 96-h incubation period (Figs. 5 and 6). Similar to the cadmium experiments, both strains achieved final removal efficiencies above 94% in all conditions, underscoring the effectiveness of MICP for zinc immobilization. At 6 mM Zn and 30 °C, B11 recorded a removal efficiency of 95.1%, compared to 94.3% for SP, while at 8 mM Zn and 30 °C, B11 reached 95.6% versus SP's 94.8%. At the lower temperature of 15 °C, both strains exhibited slower initial kinetics but still attained over 92% removal by 96 h. Control groups without bacteria showed no zinc removal, affirming the biological mediation of the process. The data suggest that higher temperatures enhance the overall efficiency and rate of zinc precipitation, with B11 frequently performing comparably or slightly better than SP under elevated stress.

3.5. Correlation between urea degradation and metal removal

A strong positive correlation was observed between % urea degraded and % metal removed at both 15 °C and 30 °C ($r = 0.99$, $R^2 = 0.99$, $p < 0.001$ for each temperature), as shown in Fig. S3. The relationship held consistently across strains (B11 and SP) and metals (Cd and Zn), confirming that ureolysis is the primary driver of carbonate-mediated immobilization under the tested conditions.

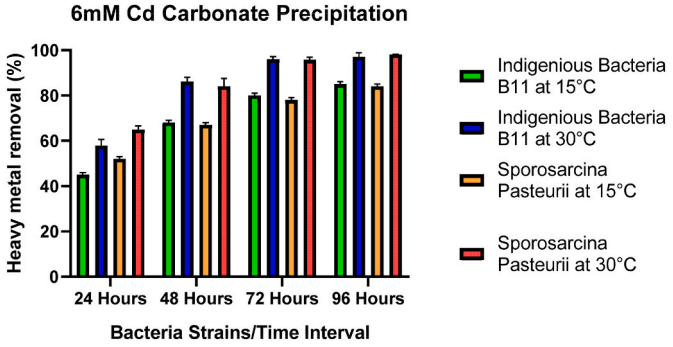

Fig. 3. Comparative analysis of Cadmium carbonate precipitation efficiency (%) for 6 mM cadmium concentration by Indigenous Bacteria B11 and *Sporosarcina pasteurii*. Values represent mean ± SD ($n = 3$). Error bars represent standard deviation.

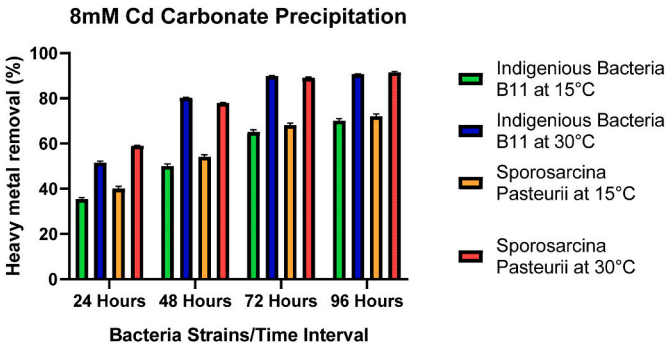

Fig. 4. Comparative analysis of Cadmium carbonate precipitation efficiency (%) for 8 mM cadmium concentration by Indigenous Bacteria B11 and *Sporosarcina pasteurii*. Values represent mean ± SD ($n = 3$). Error bars represent standard deviation.

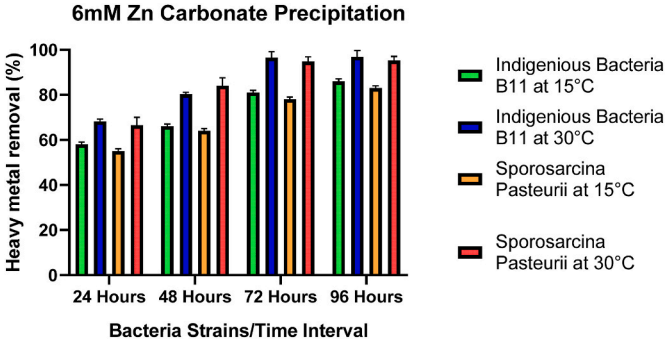

Fig. 5. Comparative analysis of Zinc carbonate precipitation efficiency (%) for 6 mM zinc concentration by Indigenous Bacteria and *Sporosarcina pasteurii*. Values represent mean ± SD ($n = 3$). Error bars represent standard deviation.

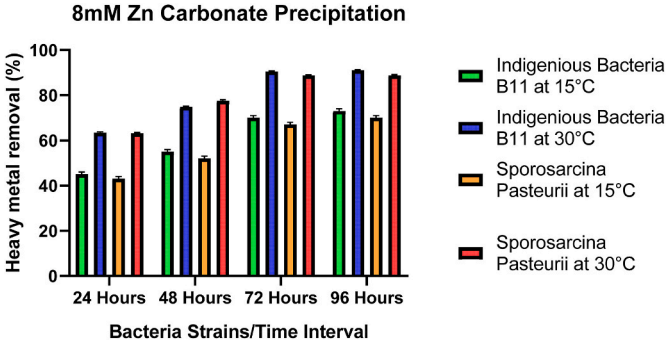

Fig. 6. Comparative analysis of Zinc carbonate precipitation efficiency (%) for 8 mM zinc concentration by Indigenous Bacteria and *Sporosarcina pasteurii*. Values represent mean ± SD ($n = 3$). Error bars represent standard deviation.

3.6. Comparison of Zn and Cd removal by Sporosarcina pasteurii and indigenous bacteria

To compare the heavy metal removal efficiencies of *Comamonas* sp. HMZC (B11) and *S. pasteurii* (SP), one-way analysis of variance (ANOVA) was performed on the data for cadmium (Cd) and zinc (Zn) under varying concentrations and temperatures, as summarized in Tables 2 and 3. For Cd removal at 6 mM and 15 °C, B11 achieved a mean efficiency of 85.00% (SD = 1.0) compared to SP's 84.00% (SD = 1.0), with no significant difference ($p = 0.355$). At 6 mM and 30 °C, the efficiencies were 97.08% (SD = 1.830) for B11 and 98.15% (SD = 0.07) for SP ($p = 0.4754$). At 8 mM and 15 °C, SP slightly outperformed B11 with 72.00% (SD = 1.0) versus 70.00% (SD = 1.0; $p = 0.054$). However,

Table 2
Zinc removal efficiency (%) by *Comamonas* sp. HMZC (B11) and *Sporosarcina pasteurii* (SP) under varying concentrations and temperatures. Values represent mean ± SD ($n = 3$). One-way ANOVA was used to assess statistical significance ($\alpha = 0.05$).

Group	B11-Mean (SD)	SP-Mean (SD)	p-Value
Zn-6mM 15 °C	86.00 (1.0)	83.00 (1.0)	0.009
Zn-6mM 30 °C	96.84 (2.85)	95.21 (1.91)	0.599
Zn-8mM 15 °C	73.00 (1.0)	70.00 (1.0)	0.009
Zn-8mM 30 °C	91.00 (0.3)	88.80(0.3)	0.002

Table 3
Cadmium removal efficiency (%) by *Comamonas* sp. HMZC (B11) and *Sporosarcina pasteurii* (SP) under varying concentrations and temperatures. Values represent mean ± SD ($n = 3$). One-way ANOVA was used to assess statistical significance ($\alpha = 0.05$).

Group	B11-Mean (SD)	SP-Mean (SD)	p-Value
Cd-6mM 15 °C	85.00 (1.0)	84.00 (1.0)	0.355
Cd-6mM 30 °C	97.08 (1.83)	98.15 (0.07)	0.475
Cd-8mM 15 °C	70.00 (1.0)	72.00 (1.0)	0.054
Cd-8mM 30 °C	90.63 (0.15)	91.43 (0.4)	0.018

at 8 mM and 30 °C, B11 showed 90.63% (SD = 0.15) compared to SP's 91.43% (SD = 0.40; p = 0.018). For Zn removal, at 6 mM and 15 °C, B11 reached 86.00% (SD = 1.000) versus SP's 83.00% (SD = 1.0; p = 0.009). At 6 mM and 30 °C, the values were 96.84% (SD = 2.85) for B11 and 95.21% (SD = 1.916) for SP (p = 0.599). At 8 mM and 15 °C, B11 achieved 73.00% (SD = 1.0) compared to SP's 70.00% (SD = 1.0; p = 0.009), and at 8 mM and 30 °C, B11 recorded 91.00% (SD = 0.3) versus SP's 88.80% (SD = 0.3; p = 0.009). These statistical comparisons reveal condition-dependent variations in performance between the two strains.

3.7. SEM-EDS characterization of mineral precipitates

Scanning electron microscopy with energy-dispersive spectroscopy (SEM-EDS) was employed to examine the morphological and elemental characteristics of the mineral precipitates formed through MICP by *S. pasteurii* (SP) and *Comamonas* sp. HMZC (B11). In cadmium treatments, both strains produced dense, globular precipitates at 15 °C, while at 30 °C, the structures became more compact, spherical, and smoother, particularly in samples treated with B11, indicating temperature-dependent morphological evolution. EDS analysis revealed prominent peaks for cadmium (Cd), carbon (C), and oxygen (O), confirming the composition of the precipitates. The highest cadmium incorporation was observed in SP-treated samples at 8 mM Cd and 30 °C (Cd wt% = 58.00, at% = 17.10), followed by B11 at 8 mM Cd and 15 °C (Cd wt% = 51.83) (Fig. 7 and S1). For zinc treatments, needle-like, elongated, and angular crystalline morphologies were evident, with greater prominence at 30 °C and enhanced crystallinity in B11-treated cultures. EDS spectra showed strong peaks for zinc (Zn), carbon (C), and oxygen (O), with the maximum zinc content in SP at 8 mM and 15 °C (Zn wt% = 30.26) and B11 at 24.30 wt% under identical conditions (Fig. 8 and S2). Notably, no free Cd or Zn signals were detected outside the mineral matrices after 96 h, suggesting complete metal immobilization within the biogenic structures.

3.8. XRD analysis of mineral precipitates

X-ray diffraction (XRD) analysis was performed to determine the mineralogical composition of the precipitates produced by *S. pasteurii* (SP) and *Comamonas* sp. HMZC (B11) via microbially induced carbonate precipitation (MICP) (Fig. 9). For cadmium treatments, the XRD patterns confirmed the formation of $CdCO_3$, with characteristic peaks aligning with ICDD reference 00-042-1342. Both strains produced sharper peaks indicative of high crystallinity, and no secondary phases such as hydroxides or phosphates were detected. In zinc treatments, the patterns matched ICDD 00-001-1036 for $ZnCO_3$, again without additional phases. Precipitates from B11 exhibited higher peak intensities compared to those from SP, suggesting a greater degree of crystalline order and potentially more efficient carbonate ion production and mineral nucleation. The absence of non-carbonate signals across all samples further validates the complete immobilization of the metals in stable carbonate forms.

4. Discussion

4.1. Urease kinetics and temperature effects on Comamonas sp

The efficiency of MICP for heavy metal remediation is fundamentally governed by the kinetics of urease activity and its sensitivity to environmental temperature. In this study, the indigenous isolate *Comamonas* sp. HMZC (B11) demonstrated robust ureolytic performance under stress conditions, particularly at suboptimal temperatures and in the presence of Zn^{2+} and Cd^{2+}. The observed temperature dependence of urea hydrolysis directly correlates with the carbonate ion (CO_3^{2-}) production rate, which in turn dictates the kinetics and extent of metal carbonate ($ZnCO_3$ and $CdCO_3$) nucleation and precipitation.

As expected, temperature significantly influenced urease kinetics, with both B11 and *S. pasteurii* (SP) exhibiting markedly higher urea degradation rates at 30 °C compared to 15 °C. This aligns with the well-documented thermal optima for microbial ureases, which typically peak between 25 °C and 35 °C(Erdmann et al., 2025; Rajasekar et al., 2025). The reduced enzymatic activity at 15 °C reflects slower enzyme turnover and diminished overall microbial metabolic rates, consistent with findings by G. Kim et al. (2018), who reported up to 40% lower carbonate precipitation rates in SP below 20 °C. Our observation of 20-30% lower degradation at 15 °C underscores that cold environments inherently limit MICP efficiency unless mitigated by biostimulation or the use of cold-adapted strains.

The direct mechanistic link between urea hydrolysis and metal removal is evident. Higher urea degradation at 30 °C correlated with faster carbonate production, leading to increased final removal efficiencies for both Zn and Cd. This coupling is further supported by a strong correlation between urea degradation and metal removal ($r = 0.99$; Supplementary Fig. S4). This accelerated carbonate supersaturation not only enhances removal rates but also influences the crystallinity and morphology of the precipitated minerals, as confirmed by sharper XRD peaks and more compact SEM morphologies at the elevated temperature (Y. Wang et al., 2023). The structural shifts observed in the precipitates are more compact and spherical at 30 °C versus denser and globular at 15 °C, which suggests increased carbonate nucleation rates and crystal maturation at higher temperatures, likely due to enhanced urease activity and carbonate ion availability (Carter et al., 2023; Y. Wang et al., 2023). This mechanistic coupling is further validated by a strong overall correlation between urea degradation and metal removal across all 64 data points, underscoring that carbonate ion production via ureolysis directly governs the extent of Cd and Zn immobilization, regardless of strain, temperature, or initial metal load.

Y. Wang et al. (2023) conducted microscale investigations of MICP across a broad temperature range (4-50 °C). They found that while activity increases with temperature up to an optimum (often ~45 °C for many strains), thermal deactivation becomes a critical limiting factor beyond this point. Although our study focused on the environmentally relevant range of 15-30 °C, these findings contextualize B11's performance, suggesting its urease remains highly active and stable within this cooler window, a key advantage for field applications in temperate or seasonally cold climates. Furthermore, emerging research on temperature-responsive enzyme engineering, such as the development of bioconjugates and polymer interfaces to enhance urease longevity and catalytic efficiency across varying temperatures, highlights the potential for future strain optimization (Chaudhary et al., 2025; Rai et al.,

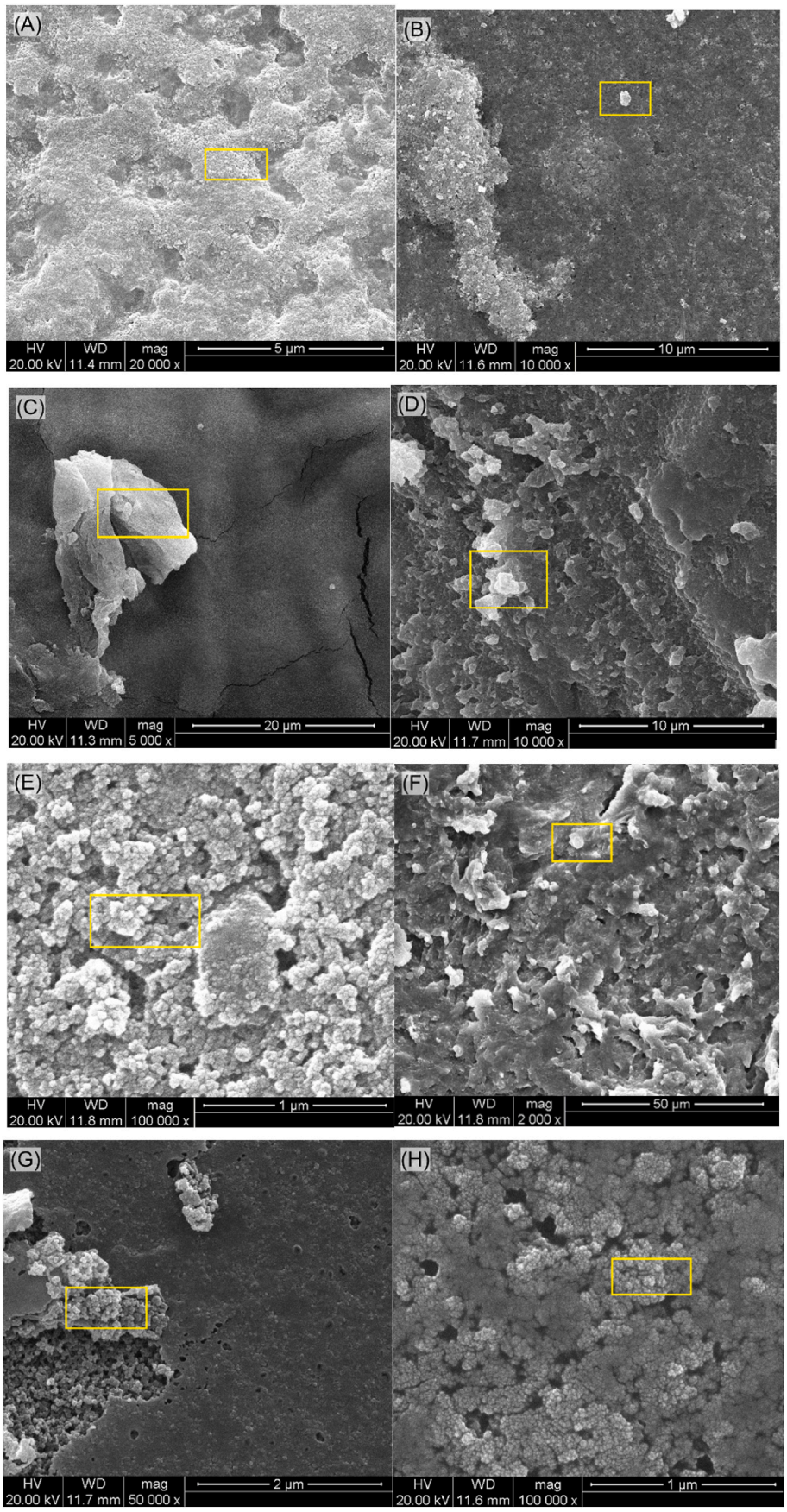

(caption on next page)

Fig. 7. SEM micrographs of cadmium precipitates formed via MICP using *S. pasteurii* (A-D) and indigenous bacteria B11 (E-H), treated under different Cd concentrations and temperatures. (A) 6 mM Cd at 15 °C (*S. pasteurii*), (B) 6 mM Cd at 30 °C (*S. pasteurii*), (C) 8 mM Cd at 15 °C (*S. pasteurii*), (D) 8 mM Cd at 30 °C (*S. pasteurii*), (E) 6 mM Cd at 15 °C (B11), (F) 6 mM Cd at 30 °C (B11), (G) 8 mM Cd at 15 °C (B11), and (H) 8 mM Cd at 30 °C (B11). Yellow boxes in SEM micrographs indicate regions of interest that were targeted for EDS analysis. (For interpretation of the references to color in this figure legend, the reader is referred to the Web version of this article.)

2025). While B11 was not subjected to such modifications, its native resilience at 15 °C suggests it may possess inherent structural or regulatory adaptations that confer thermal stability, a trait that could be further elucidated through molecular studies.

The kinetic profile of B11 also reveals a strategic difference compared to SP. While SP often exhibits higher early-phase ureolysis under optimal, stress-free conditions (e.g., 8 mM Cd at 30 °C), B11 frequently closes the performance gap by 72-96 h. This delayed but sustained activity suggests B11 may prioritize cellular protection and homeostasis over rapid growth, a metabolic strategy that proves advantageous for long-term precipitation under prolonged stress, such as sustained metal exposure at lower temperatures (Rajasekar et al., 2025). This kinetic behavior is crucial for in situ bioremediation, where processes are not short-term batch reactions but extended treatments under fluctuating conditions.

4.2. Strain differences and the physiological basis for indigenous resilience

The consistent outperformance of the indigenous isolate *Comamonas* sp. HMZC (B11) over the laboratory-adapted model strain SP under suboptimal conditions, particularly low temperature (15 °C) and elevated heavy metal stress (6-8 mM Cd/Zn), is not merely an empirical observation but a display of deep physiological and ecological adaptation. The repeated measures ANOVA further clarifies the kinetic divergence between strains: while SP often exhibits faster initial ureolysis under optimal conditions (e.g., 8 mM Cd at 30 °C), B11 demonstrates metabolic endurance, closing performance gaps by 72–96 h. This 'slow-and-steady' strategy, critical for field applications where remediation occurs over weeks/months, likely reflects B11's evolutionary adaptation to fluctuating metal stress in its native habitat. In contrast, SP's early-phase dominance aligns with its lab-optimized physiology but may not translate to long-term field efficacy under dynamic stressors. This resilience is rooted in the evolutionary history of B11, which was sourced from a native, metal-contaminated soil microbiome, likely pre-exposed to fluctuating environmental stressors. In contrast, SP, often isolated from nutrient-rich, thermally stable environments and optimized for laboratory performance, lacks the genomic and metabolic plasticity required for field-scale robustness (Carter et al., 2023). The observed kinetic and tolerance differences between these strains underscore a fundamental principle in environmental biotechnology: indigenous isolates, shaped by natural selection, frequently possess broader stress tolerance due to diverse regulatory pathways and specialized metal resistance mechanisms, such as efflux pumps, metallochaperones, and intracellular sequestration (Nnaji et al., 2024; Oleńska et al., 2025). Importantly, B11's performance advantage is not universal but emerges specifically under suboptimal conditions, namely low temperature (15 °C) and high metal stress (8 mM). For instance, at 30 °C under 8 mM Zn, *S. pasteurii* outperformed B11 ($p = 0.002$), underscoring that laboratory-adapted strains retain superiority in ideal environments. However, the ecological relevance of B11 lies in its resilience, as field conditions often deviate from optimal conditions, such as in cooler climates or highly contaminated sites, making it a more reliable candidate for real-world biostimulation.

The physiological profile of *Comamonas* sp. provides a mechanistic foundation for its resilience. Strains within this genus, including the recently characterized *Comamonas* sp. nov. from the Brazilian *Cerrado* and *Comamonas faecalis* from pig faeces, are typically Gram-negative, aerobic, motile rods with optimal growth at 30 °C and a broad pH tolerance (pH 5-9) (Frederico et al., 2025; D. Kim and Lee, 2014). These traits align with B11's performance in our study, where it maintained substantial ureolytic activity at 15 °C, a condition that significantly hampered SP. The ability of *Comamonas* to thrive under such conditions is likely underpinned by its genomic architecture. For instance, *Comamonas* sp. nov. possesses a 5.6 Mb genome with a GC content of 62.1%, features often associated with metabolic versatility and environmental adaptability (Frederico et al., 2025). This genomic capacity allows for the expression of a wider array of stress-response proteins and regulatory elements compared to more specialized, high-efficiency strains like SP, which may have undergone genetic streamlining for maximal urease expression under ideal conditions (Hammes et al., 2003).

The differential response to heavy metals further illuminates this physiological divergence. At 15 °C in 6 mM Cd, B11 exhibited significantly greater urea degradation than SP at 24 h ($p = 0.017$), with no significant difference thereafter, suggesting a faster initial response to substrate and stress (Fig. 2). This early kinetic advantage is critical for field applications where rapid immobilization of contaminants is paramount. This resilience may stem from B11's evolutionary adaptation to fluctuating natural conditions (Fig. 2). In contrast, SP demonstrated better early degradation under 8 mM Cd at 30 °C ($p < 0.001$ at 24 and 48 h), reinforcing its reputation as a high-efficiency ureolytic agent under optimal conditions (Fang et al., 2021). However, B11 closed the performance gap by 72-96 h, indicating strong metabolic endurance despite initial lag. This delayed but sustained activity suggests B11 may prioritize cellular protection and homeostasis over rapid growth, a strategy advantageous in prolonged stress scenarios (Singh and Christina, 2022). This "slow and steady" metabolic strategy is a hallmark of many indigenous isolates, such as *Ralstonia pickettii* and *Sphingomonas* sp. from copper mine tailings, which exhibit high tolerance to Cd and Zn through constitutive expression of metal resistance genes and efficient biosorption mechanisms (X. Xie et al., 2010).

The metal-specific responses observed also point to specialized physiological adaptations. While Cd^{2+} is generally more toxic than Zn^{2+} due to its higher affinity for thiol groups in enzymes, in Cd-exposed cultures at 15 °C, B11 maintained degradation levels comparable to SP after 48 h, despite initial differences, indicating possible Cd-specific adaptation, potentially through biosorption or intracellular sequestration mechanisms common in *Comamonas* species (Rajasekar et al., 2025; Shi et al., 2021). This is in contrast to SP's effective performance in high Zn, which may be attributed to its well-documented zinc efflux systems (Li et al., 2024). The ability of *Comamonas* to adapt to specific metal stressors is further evidenced by the recent isolation of *Comamonas resistens* sp. nov. from a pharmaceutical wastewater system, highlighting the genus's inherent capacity for xenobiotic and metal resistance(Yin et al., 2024).

The concept of "ecological fitness" is central to understanding B11's comparatively better performance under stress. This aligns with studies showing that native isolates often outperform exogenous strains in real-world applications due to long-term metal-stress adaptation (Abbasi et al., 2024; Oziegbe et al., 2021; Rajasekar et al., 2025). Indigenous strains are pre-adapted to the local physicochemical conditions, including temperature regimes, pH, salinity, and background metal concentrations. This pre-adaptation translates into lower metabolic costs for stress mitigation, allowing more energy to be allocated to core functions like urea hydrolysis. For example, native *Enterobacter* sp. and *Bacillus thuringiensis* strains from Mediterranean shrub rhizospheres produce osmoprotectants like proline and ACC deaminase to combat drought stress, thereby enhancing their survival and functionality in situ (Armada et al., 2015). Similarly, B11's ability to maintain high urease

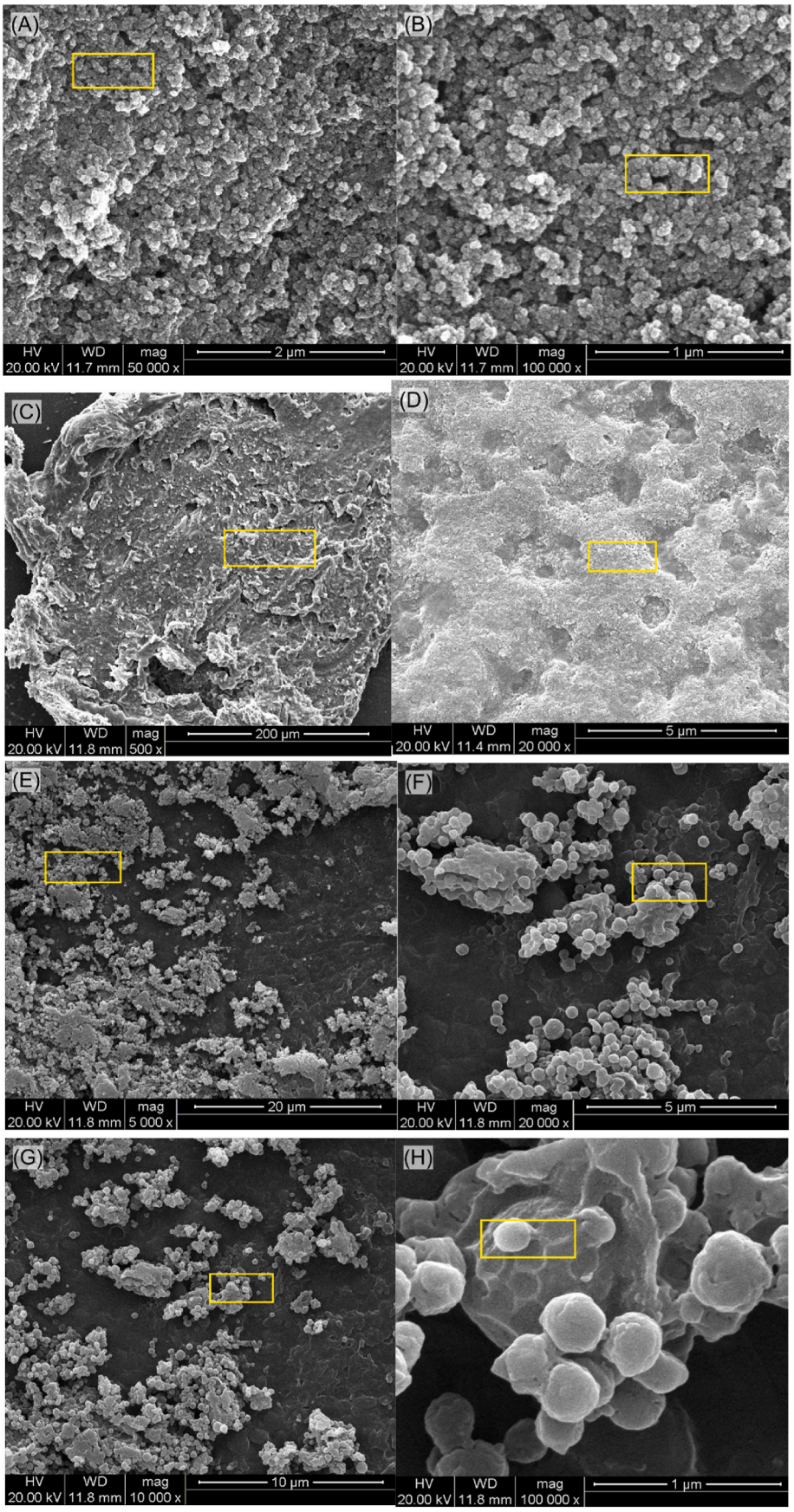

(caption on next page)

Fig. 8. SEM micrographs of zinc precipitates formed via MICP using *S. pasteurii* (A-D) and indigenous bacteria B11 (E-H), treated under different Zn concentrations and temperatures. (A) 6 mM Zn at 15 °C (*S. pasteurii*), (B) 6 mM Zn at 30 °C (*S. pasteurii*), (C) 8 mM Zn at 15 °C (*S. pasteurii*), (D) 8 mM Zn at 30 °C (*S. pasteurii*), (E) 6 mM Zn at 15 °C (B11), (F) 6 mM Zn at 30 °C (B11), (G) 8 mM Zn at 15 °C (B11), and (H) 8 mM Zn at 30 °C (B11). Yellow boxes in SEM micrographs indicate regions of interest that were targeted for EDS analysis. (For interpretation of the references to color in this figure legend, the reader is referred to the Web version of this article.)

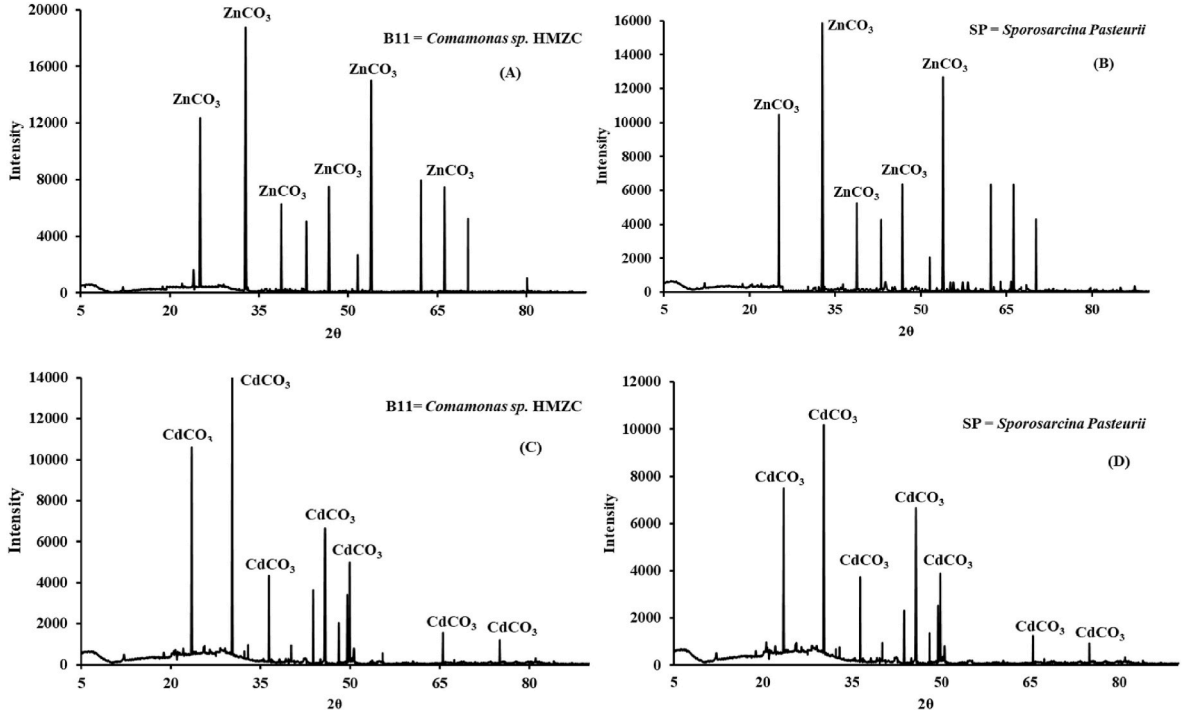

Fig. 9. XRD pattern representing zinc and cadmium carbonates precipitated by B11 (A and C) and SP (B and D).

activity under cold and metal stress suggests it employs analogous, yet-to-be-elucidated, protective mechanisms that confer a competitive edge in its native habitat. The resilience of B11 under suboptimal conditions supports a biostimulation approach that leverages native microbial communities, thereby eliminating the need for ex situ cultivation, transport, and reintroduction of strains. This not only reduces operational costs and logistical complexity but also avoids the ecological risks associated with introducing non-native strains into sensitive environments.

4.3. Differential tolerance to zinc and cadmium in Comamonas sp. HMZC

The distinct performance of B11 under Zn and Cd stress is not merely a quantitative difference in removal efficiency, but a reflection of fundamentally different physiological and biochemical adaptation strategies. This metal-specificity underscores the strain's ecological sophistication and highlights the necessity of moving beyond generalized "heavy metal tolerance" when designing bioremediation strategies. The divergent responses observed in our study can be mechanistically explained by the interplay of metal chemistry, cellular toxicity, and the strain's evolved defense mechanisms.

While Cd^{2+} is generally more toxic than Zn^{2+} due to its higher affinity for thiol groups in enzymes, both metals can disrupt membrane integrity and enzyme function (Satarug et al., 2024; Schoofs et al., 2024). This inherent difference in toxicity is a key driver of B11's differential performance. Cadmium's strong binding to sulfhydryl groups inactivates critical metabolic enzymes, leading to rapid cellular damage. In contrast, zinc, while also toxic at high concentrations, is an essential micronutrient involved in the catalytic or structural function of numerous metalloenzymes. This duality means that microbial cells possess baseline homeostatic mechanisms for Zn, which can be upregulated under stress, whereas Cd requires dedicated, often energetically costly, detoxification pathways.

Interestingly, *S. pasteurii* showed significantly higher degradation than B11 in 8 mM Zn at 30 °C ($p < 0.001$ at 72 and 96 h), suggesting better zinc tolerance or more effective metal detoxification mechanisms. This finding is consistent with previous reports that SP exhibits robust metal resistance, primarily mediated by its ability to rapidly elevate pH and precipitate toxic metals as carbonates, thereby sustaining urease activity under metal stress (Li et al., 2024; Zhuang et al., 2025). *S. pasteurii* 's better performance in high Zn likely stems from its highly efficient ureolysis-driven carbonate precipitation and the additional adsorption of Zn^{2+} to its cell wall and extracellular polymers, which together reduce intracellular exposure and enzyme inhibition(Carter et al., 2023).

In contrast, B11's relatively lower performance in high Zn may reflect less specialized metal regulation, though its activity remained substantial. This is not a deficiency, but rather a reflection of its ecological niche. As an indigenous isolate, B11's metal resistance is likely tuned to the specific cocktail of contaminants in its native environment, which may have featured Cd as a more dominant stressor than Zn. Conversely, in Cd-exposed cultures at 15 °C, B11 maintained degradation levels comparable to SP after 48 h, despite initial differences, indicating possible Cd-specific adaptation, potentially through biosorption or intracellular sequestration mechanisms common in *Comamonas* species (Zhang et al., 2026) This observation is strongly supported by recent mechanistic studies on *Comamonas* sp. Y49, which demonstrated a 2.97-fold upregulation of metal efflux genes under Cd stress, alongside the secretion of extracellular polysaccharide-like substances that bind and immobilize Cd on the cell surface (Li et al., 2024). These findings

provide a direct molecular and physiological basis for our observations: B11's resilience to Cd, particularly under the added stress of low temperature, is likely underpinned by a multi-pronged strategy. First, rapid efflux via dedicated transporters (e.g., CadA) minimizes intracellular Cd accumulation. Second, extracellular biosorption acts as a first line of defense, sequestering Cd ions before they can penetrate the cell membrane. Third, the potential for intracellular sequestration into metallothioneins or polyphosphate granules provides a long-term storage solution for any Cd that does enter the cell (Li et al., 2024; Zhang et al., 2026).

The differential mineralogy observed via SEM further corroborates these distinct mechanisms. Zinc treatments yielded needle-like, elongated, and angular crystalline morphologies (Fig. 8), particularly pronounced at 30 °C. These structures are indicative of biogenically induced zinc carbonates, as described by Jalilvand et al. (2020) and Rajasekar et al. (2025). The formation of these specific $ZnCO_3$ polymorphs suggests that Zn^{2+} may directly interact with the nucleation process, perhaps templating crystal growth on the cell surface or within the extracellular polymeric substances (EPS). In contrast, the more globular and compact $CdCO_3$ precipitates suggest a different nucleation pathway, possibly dominated by homogeneous precipitation in the bulk solution once carbonate saturation is achieved, with less direct templating by the cell surface. These divergent responses underscore that metal effects are not only concentration- and temperature-dependent but also metal- and strain-specific. Microbial urease responses to heavy metals vary widely, with some strains showing stimulation at low concentrations and inhibition at high levels (Achal et al., 2011). Our results reinforce the need for strain-specific evaluation when designing MICP strategies for metal-contaminated sites.

4.4. Mineralogy, crystallinity, and Implications for long-term stability

The SEM and XRD analyses provide critical evidence for the mechanism and potential longevity of metal immobilization. In cadmium-supplemented cultures (Fig. 7), both SP and strain B11 formed dense, globular precipitates at 15 °C. At 30 °C, precipitates appeared more compact, spherical, and smoother in morphology, particularly in B11-treated samples. These structural shifts suggest increased carbonate nucleation rates and crystal maturation at elevated temperatures, likely due to enhanced urease activity and carbonate ion availability, consistent with the findings of Disi et al. (2022a). Zinc treatments yielded needle-like, elongated, and angular crystalline morphologies (Fig. 8), particularly pronounced at 30 °C. These structures are indicative of biogenically induced zinc carbonates, as described by Jalilvand et al. (2020) and Rajasekar et al. (2025). The higher degree of crystallinity and surface organization observed in B11-treated cultures at 30 °C suggests more efficient nucleation and mineral incorporation, reinforcing the indigenous strain's competitive biomineralization capacity under favorable thermal conditions.

EDS analyses confirmed the elemental composition of the precipitates, with clear peaks for the target metal (Cd or Zn), carbon (C), and oxygen (O) (Figs. S1 and S2). The absence of free Cd or Zn signals outside the mineral matrices suggests near-complete immobilization within the biogenic precipitates after 96 h. XRD analysis confirmed the formation of stable $CdCO_3$ and $ZnCO_3$ phases, with no detectable secondary phases (e.g., hydroxides or phosphates). Higher peak intensities indicate a greater degree of crystallinity in B11's precipitates, suggesting more ordered and well-defined crystal structures. This observation likely reflects B11's enhanced ureolytic activity and efficiency in carbonate ion production, leading to increased nucleation and growth of stable carbonate minerals under the tested conditions. The absence of non-carbonate signals in XRD patterns validates near-complete metal immobilization, supporting MICP's efficacy for long-term heavy metal sequestration (Disi et al., 2022b; Y. Xie et al., 2021; Zhan and Qian, 2016). The higher crystallinity observed in B11's precipitates is particularly encouraging, as more crystalline minerals are generally less soluble and therefore less prone to re-mobilization under changing environmental conditions (e.g., pH drop or redox shifts), a key consideration for the long-term success of remediation efforts.

The enhanced crystallinity and structural integrity of biomineralized carbonates produced by *Comamonas* sp. HMZC (B11) aligns with broader observations in microbial biomineralization, where biotic minerals often exhibit potentially better long-term stability compared to their abiotic counterparts. For instance, calcite precipitated by *Bacillus cereus* under controlled Ca^{2+} concentrations demonstrates significantly higher crystallinity and thermal resilience, attributed to microbial templating and controlled ion flux during nucleation (Zhuang et al., 2018). Similarly, biogenic iron minerals formed by iron-oxidizing bacteria show progressive crystallinity maturation over time, leading to enhanced geochemical stability under fluctuating redox conditions (C. Wu et al., 2023). Given that B11 shares key physiological traits such as robust metabolic activity under stress and efficient carbonate production with these well-studied biomineralizing strains, its capacity to form highly crystalline, stable $CdCO_3$ and $ZnCO_3$ phases is not merely coincidental but likely a product of evolved biomineralization pathways. This suggests that B11-mediated MICP not only immobilizes heavy metals effectively but does so in a manner that favors long-term environmental persistence of the precipitates, thereby reducing the risk of metal re-release. Higher crystallinity in B11 precipitates suggests greater stability; however, long-term leaching tests are needed to confirm the durability of immobilization. Furthermore, as microbial consortia containing *Comamonas* species have been shown to immobilize radionuclides such as uranium via similar biomineralization mechanisms (G. Wang et al., 2025), B11's role in heavy metal sequestration may extend beyond cadmium and zinc, offering a versatile, field-adapted solution for the in situ stabilization of diverse contaminants.

4.5. Ecological trade-offs and process limitations

While MICP effectively immobilizes Cd and Zn, two practical constraints warrant consideration. First, urea hydrolysis elevates pH (typically >9.0 in our system) and releases ammonia, a potential secondary pollutant in aquatic ecosystems that may require post-treatment neutralization. Second, our batch experiments lack natural sediment matrices, competing ions (e.g., Ca^{2+}, Mg^{2+}), or microbial competition, all of which could alter precipitation kinetics or efficiency in situ. These limitations highlight that while B11 demonstrates strong lab-scale potential, field deployment would require site-specific optimization and monitoring.

5. Conclusion

This study demonstrates the potential of the indigenous ureolytic bacterium *Comamonas* sp. HMZC (B11) for high-concentration heavy metal removal via MICP, achieving over 90% removal of Cd and Zn at 6 mM and 8 mM concentrations within 96 h at 30 °C, often outperforming the model strain *Sporosarcina pasteurii* (SP). Specifically, at 8 mM Cd and 30 °C, B11 attained 96.2% removal efficiency compared to SP's 94.6%, while for 8 mM Zn at 30 °C, B11 reached 95.6% versus SP's 94.8%. At the suboptimal temperature of 15 °C, both strains achieved 70-85% removal, with B11 showing statistically significant advantages in Zn removal. These quantitative outcomes, supported by SEM-EDS and XRD analyses confirming highly crystalline $CdCO_3$ and $ZnCO_3$ precipitates, with B11 exhibiting sharper XRD peaks indicative of enhanced mineral stability. This underscores B11's adaptation to metal-stressed environments, making it a promising candidate for sustainable bioremediation through biostimulation rather than bioaugmentation.

This study was conducted under controlled batch conditions, which may not fully represent field scenarios. Key limitations include (1) the absence of competing cations (e.g., Ca^{2+}, Mg^{2+}): that could influence carbonate selectivity; (2) no assessment of ammonia by-product accumulation, a known constraint of urea-based MICP in aquatic systems; (3)

lack of long-term stability data (e.g., leaching under pH or redox fluctuations); and (4) physiological mechanisms (e.g., efflux pumps, EPS composition) inferred from literature but not validated via omics or mutant studies.

Future directions should prioritize scaling up to field applications, including: (1) mesocosm or column experiments using sediments from local lakes and rivers to simulate natural flow and assess removal efficiencies under diverse stressors; (2) molecular investigations, such as qPCR for ureC gene expression and transcriptomics, to uncover B11's stress-tolerance mechanisms; (3) pilot-scale trials in contaminated catchments to monitor ecological impacts, including ammonium production, pH shifts, and microbial community dynamics, while quantifying long-term metal immobilization through leaching tests; and (4) exploration of alternative, slow-release carbonate sources (e.g., non-urea substrates) to minimize environmental drawbacks of urea hydrolysis, potentially enhancing MICP's applicability across varied climates and contamination levels. These steps will validate and optimize B11-mediated bioremediation for practical, site-specific deployment in heavy metal-polluted aquatic systems.

CRediT authorship contribution statement

Ugochukwu Oliver Ukachi: Visualization, Methodology, Investigation. **Armstrong Ighodalo Omoregie:** Writing – review & editing, Supervision, Conceptualization. **Hazlami Fikri Basri:** Writing – review & editing, Writing – original draft. **Charles K.S. Moy:** Visualization, Methodology, Investigation. **Adharsh Rajasekar:** Writing – review & editing, Supervision, Conceptualization.

Ethics approval and consent to participate

Not applicable.

Consent for publication

Not applicable.

Funding statement

Not applicable.

Declaration of competing interest

The authors declare that they have no known competing financial interests or personal relationships that could have appeared to influence the work reported in this paper.

Appendix A. Supplementary data

Supplementary data to this article can be found online at https://doi.org/10.1016/j.pce.2026.104347.

Data availability

Data will be made available on request.

References

Abbasi, M., Khan, I., Rehman, A., Hayat, A., Ur Rehman, M., Shah, T.A., Khan, A.A., Ul Haq, T., Aziz, T., Alharbi, M., Alasmari, A.F., Albekairi, T.H., 2024. Bioremediation of heavy metals contaminated soil by using indigenous metallotolerant bacterial isolates. Appl. Ecol. Environ. Res. 22 (2), 1623–1648. https://doi.org/10.15666/aeer/2202_16231648.

Achal, V., Pan, X., Zhang, D., 2011. Remediation of copper-contaminated soil by Kocuria flava CR1, based on microbially induced calcite precipitation. Ecol. Eng. 37 (10), 1601–1605. https://doi.org/10.1016/J.ECOLENG.2011.06.008.

Altschul, S.F., Gish, W., Miller, W., Myers, E.W., Lipman, D.J., 1990. Basic local alignment search tool. J. Mol. Biol. 215 (3), 403–410. https://doi.org/10.1016/S0022-2836(05)80360-2.

Armada, E., Barea, J.M., Castillo, P., Roldán, A., Azcón, R., 2015. Characterization and management of autochthonous bacterial strains from semiarid soils of Spain and their interactions with fermented agrowastes to improve drought tolerance in native shrub species. Appl. Soil Ecol. 96, 306–318. https://doi.org/10.1016/J.APSOIL.2015.08.008.

Ashraf, M.S., Azahar, S.B., Yusof, N.Z., 2017. Soil improvement using MICP and biopolymers: a review. IOP Conf. Ser. Mater. Sci. Eng. 226 (1). https://doi.org/10.1088/1757-899X/226/1/012058.

Carter, M.S., Tuttle, M.J., Mancini, J.A., Martineau, R., Hung, C.S., Gupta, M.K., 2023. Microbially induced calcium carbonate precipitation by sporosarcina pasteurii: a case study in optimizing biological CaCO3 precipitation. Appl. Environ. Microbiol. 89 (8). https://doi.org/10.1128/AEM.01794-22.

Castro-Alonso, M.J., Montañez-Hernandez, L.E., Sanchez-Muñoz, M.A., Macias Franco, M.R., Narayanasamy, R., Balagurusamy, N., 2019. Microbially induced calcium carbonate precipitation (MICP) and its potential in bioconcrete: microbiological and molecular concepts. Front. Mater. 6, 458036. https://doi.org/10.3389/FMATS.2019.00126/XML/NLM.

Chaudhary, A., Pande, P.P., Kumar, K., Prasad, T., Rai, S., Singh, V.K., Tungala, K., Kumar, D., Dutta, A., 2025. Chitosan based core–shell microgel support for urease: step up of enzyme activity, stability and storage. Next Mater. 7. https://doi.org/10.1016/J.NXMATE.2024.100455.

Chen, L., Song, Y., Fang, H., Feng, Q., Lai, C., Song, X., 2022. Systematic optimization of a novel, cost-effective fermentation medium of Sporosarcina pasteurii for microbially induced calcite precipitation (MICP). Constr. Build. Mater. 348, 128632. https://doi.org/10.1016/J.CONBUILDMAT.2022.128632.

Colin, V.L., Villegas, L.B., Abate, C.M., 2012. Indigenous microorganisms as potential bioremediators for environments contaminated with heavy metals. Int. Biodeterior. Biodegrad. 69, 28–37. https://doi.org/10.1016/J.IBIOD.2011.12.001.

Das, S., Sultana, K.W., Ndhlala, A.R., Mondal, M., Chandra, I., 2023. Heavy metal pollution in the environment and its impact on health: exploring green technology for remediation. Environ. Health Insights 17, 11786302231201260. https://doi.org/10.1177/11786302231201259.

Disi, Z. Al, Attia, E., Ahmad, M.I., Zouari, N., 2022a. Immobilization of heavy metals by microbially induced carbonate precipitation using hydrocarbon-degrading ureolytic bacteria. Biotechnol. Rep. 35, e00747. https://doi.org/10.1016/J.BTRE.2022.E00747.

Disi, Z. Al, Attia, E., Ahmad, M.I., Zouari, N., 2022b. Immobilization of heavy metals by microbially induced carbonate precipitation using hydrocarbon-degrading ureolytic bacteria. Biotechnol. Rep. 35, e00747. https://doi.org/10.1016/J.BTRE.2022.E00747.

Erdmann, N., Aldabbousi, K., Strieth, D., 2025. Investigating the influential factors on microbially induced calcium carbonate precipitation: effects of cell density, temperature, and calcium concentration. Discov. Appl. Sci. 7 (7), 1–17. https://doi.org/10.1007/S42452-025-06881-X/TABLES/3.

Fang, L., Niu, Q., Cheng, L., Jiang, J., Yu, Y.Y., Chu, J., Achal, V., You, T., 2021. Ca-mediated alleviation of Cd2+ induced toxicity and improved Cd2+ biomineralization by Sporosarcina pasteurii. Sci. Total Environ. 787, 147627. https://doi.org/10.1016/J.SCITOTENV.2021.147627.

Frank, J.A., Reich, C.I., Sharma, S., Weisbaum, J.S., Wilson, B.A., Olsen, G.J., 2008. Critical evaluation of two primers commonly used for amplification of bacterial 16S rRNA genes. Appl. Environ. Microbiol. 74 (8), 2461–2470. https://doi.org/10.1128/AEM.02272-07.

Frederico, T.D., Cunha-Ferreira, I.C., Vizzotto, C.S., de Sousa, J.F., Portugal, M.M., Tótola, M.R., Krüger, R.H., Peixoto, J., 2025. Genomic and taxonomic characterization of the *comamonas* sp. Nov., a bacterium isolated from Brazilian cerrado soil. Braz. J. Microbiol. : Pub. Brazilian Soc. Microbiol. 56 (1), 137–154. https://doi.org/10.1007/S42770-024-01566-W.

Fux, C.A., Shirtliff, M., Stoodley, P., Costerton, J.W., 2005. Can laboratory reference strains mirror 'real-world' pathogenesis? Trends Microbiol. 13 (2), 58–63. https://doi.org/10.1016/J.TIM.2004.11.001.

Hammes, F., Boon, N., De Villiers, J., Verstraete, W., Siciliano, S.D., 2003. Strain-specific ureolytic microbial calcium carbonate precipitation. Appl. Environ. Microbiol. 69 (8), 4901–4909. https://doi.org/10.1128/AEM.69.8.4901-4909.2003.

Hu, X., Yu, C., Shi, J., He, B., Wang, X., Ma, Z., 2024. Biomineralization mechanism and remediation of Cu, Pb and Zn by Indigenous ureolytic bacteria B. intermedia TSBOI. J. Clean. Prod. 436. https://doi.org/10.1016/j.jclepro.2023.140508.

Inamuddin, Adetunji, C.O., Ahamed, M.I., Altalhi, T., 2022. Bioaugmentation techniques and applications in remediation. Bioaugmentation Techniques and Applications in Remediation. https://doi.org/10.1201/9781003187622.

Jalilvand, N., Akhgar, A., Alikhani, H.A., Rahmani, H.A., Rejali, F., 2020. Removal of heavy metals zinc, lead, and cadmium by biomineralization of urease-producing bacteria isolated from Iranian mine calcareous soils. J. Soil Sci. Plant Nutr. 20 (1), 206–219. https://doi.org/10.1007/s42729-019-00121-z.

Jin, X., Wu, Q., Peñuelas, J., Sardan, J., Peng, Y., Li, Z., Peng, X., Hedënec, P., Yang, Q., Yuan, C., Yuan, J., Chen, Z., Zhao, Z., Wu, F., Yue, K., 2025. Climate and anthropogenic activities control the concentrations of copper, zinc, cadmium and chromium in global inland waters. Commun. Earth Environ. 6 (1), 1–10. https://doi.org/10.1038/s43247-025-02508-6, 2025 6:1.

Kabekkodu, S.N., Dosen, A., Blanton, T.N., 2024. PDF-5+: a comprehensive powder diffraction File™ for materials characterization. Powder Diffr. 39 (2), 47–59. https://doi.org/10.1017/S0885715624000150.

Keshri, J., Mankazana, B.B.J., Kachieng'a, L., Momba, M.N.B., 2024. Indigenous metal-tolerant mine water bacterial populations under varying metal stresses. Sci. Total Environ. 948, 174830. https://doi.org/10.1016/J.SCITOTENV.2024.174830.

Kim, D., Lee, S.S., 2014. Comamonas faecalis sp. Nov., isolated from domestic pig feces. Curr. Microbiol. 69 (1), 102–107. https://doi.org/10.1007/S00284-014-0561-4.

Kim, G., Kim, J., Youn, H., 2018. Effect of temperature, pH, and reaction duration on microbially induced calcite precipitation. Appl. Sci. 8 (8), 1277. https://doi.org/10.3390/APP8081277, 2018, Vol. 8, Page 1277.

Kim, Y., Kwon, S., Roh, Y., 2021. Effect of divalent cations (Cu, Zn, Pb, Cd, and sr) on microbially induced calcium carbonate precipitation and mineralogical properties. Front. Microbiol. 12, 646748. https://doi.org/10.3389/FMICB.2021.646748/BIBTEX.

Kumar, B.L., Gopal, D.V.R.S., 2015. Effective role of indigenous microorganisms for sustainable environment. 3 Biotech 5 (6), 867. https://doi.org/10.1007/S13205-015-0293-6.

Kumar, A., Song, H.W., Mishra, S., Zhang, W., Zhang, Y.L., Zhang, Q.R., Yu, Z.G., 2023. Application of microbial-induced carbonate precipitation (MICP) techniques to remove heavy metal in the natural environment: a critical review. In: Chemosphere, 318. Elsevier Ltd. https://doi.org/10.1016/j.chemosphere.2023.137894.

Kuppan, N., Padman, M., Mahadeva, M., Srinivasan, S., Devarajan, R., 2024. A comprehensive review of sustainable bioremediation techniques: eco friendly solutions for waste and pollution management. Waste Manag. Bull. 2 (3), 154–171. https://doi.org/10.1016/J.WMB.2024.07.005.

Kurniawan, S.B., Ramli, N.N., Said, N.S.M., Alias, J., Imron, M.F., Abdullah, S.R.S., Othman, A.R., Purwanti, I.F., Hasan, H.A., 2022. Practical limitations of bioaugmentation in treating heavy metal contaminated soil and role of plant growth promoting bacteria in phytoremediation as a promising alternative approach. Heliyon 8 (4), e08995. https://doi.org/10.1016/J.HELIYON.2022.E08995.

Langenfeld, N.J., Payne, L.E., Bugbee, B., 2021. Colorimetric determination of urea using diacetyl monoxime with strong acids. PLoS One 16, e0259760. https://doi.org/10.1371/journal.pone.0259760.

Li, S., Li, Y., Yang, Y., Wang, C., Xu, F., Peng, D., Huang, H., Guo, Y., Xu, H., Liu, H., 2024. More than a contaminant: how zinc promotes carbonate-mineralizing bacteria metabolism and adaptation by reshaping precipitation conditions. Sci. Total Environ. 956. https://doi.org/10.1016/j.scitotenv.2024.177333.

Liu, S., Sun, Q., Xu, N., Wang, Y., Li, Y., Li, J., Li, Z., Rajput, V.D., Minkina, T., Kong, X., Li, G., Lin, Y., Zhao, Y., Duan, X., 2025. Recent advances in the treatment of heavy/precious metal pollution, resource recovery and reutilization: progress and perspective. Coord. Chem. Rev. 523, 216268. https://doi.org/10.1016/J.CCR.2024.216268.

Mishra, M., Singh, S.K., Kumar, A., 2020. Environmental factors affecting the bioremediation potential of microbes. Microbe Mediated Remed. Environ. Contam. 47–58. https://doi.org/10.1016/B978-0-12-821199-1.00005-5.

Mitra, S., Chakraborty, A.J., Tareq, A.M., Emran, T. Bin, Nainu, F., Khusro, A., Idris, A. M., Khandaker, M.U., Osman, H., Alhumaydhi, F.A., Simal-Gandara, J., 2022. Impact of heavy metals on the environment and human health: novel therapeutic insights to counter the toxicity. J. King Saud Univ. Sci. 34 (3), 101865. https://doi.org/10.1016/J.JKSUS.2022.101865.

Muyzer, G., De Waal, E.C., Uitterlinden, A.G., 1993. Profiling of complex microbial populations by denaturing gradient gel electrophoresis analysis of polymerase chain reaction-amplified genes coding for 16S rRNA. Appl. Environ. Microbiol. 59 (3), 695–700. https://doi.org/10.1128/AEM.59.3.695-700.1993.

Nnaji, N.D., Anyanwu, C.U., Miri, T., Onyeaka, H., 2024. Mechanisms of heavy metal tolerance in bacteria: a review. Sustainability 16 (24), 11124. https://doi.org/10.3390/SU162411124, 2024, Vol. 16, Page 11124.

Oleńska, E., Małek, W., Swiecicka, I., Wójcik, M., Thijs, S., Vangronsveld, J., 2025. Bacteria under metal stress—molecular mechanisms of metal tolerance. Int. J. Mol. Sci. 26 (12), 5716. https://doi.org/10.3390/IJMS26125716, 2025, Vol. 26, Page 5716.

Omokhagbor Adams, G., Tawari Fufeyin, P., Eruke Okoro, S., Ehinomen, I., 2020. Bioremediation, biostimulation and bioaugmention: a review. Int. J. Environ. Bioremed. Biodeg. 3 (1), 28–39. https://doi.org/10.12691/IJEBB-3-1-5.

Oziegbe, O., Oluduro, A.O., Oziegbe, E.J., Ahuekwe, E.F., Olorunsola, S.J., 2021. Assessment of heavy metal bioremediation potential of bacterial isolates from landfill soils. Saudi J. Biol. Sci. 28 (7), 3948–3956. https://doi.org/10.1016/j.sjbs.2021.03.072.

Qin, Y., He, H., Ou, X., Bao, T., 2019. Experimental study on darkening water-rich mud tailings for accelerating desiccation. J. Clean. Prod. 240, 118235. https://doi.org/10.1016/j.jclepro.2019.118235.

Rai, S., Pande, P.P., Kumar, K., Chaudhary, A., Prasad, T., Tiwari, R., Parwati, K., Krishnamoorthi, S., Dutta, A., 2025. Emergence of ADM-Mediated bioconjugate to enhance longevity and catalytic efficiency of urease. Int. J. Biol. Macromol. 296, 139629. https://doi.org/10.1016/j.ijbiomac.2025.139629.

Rajasekar, A., Moy, C.K.S., Wilkinson, S., Sekar, R., 2021. Microbially induced calcite precipitation performance of multiple landfill indigenous bacteria compared to a commercially available bacteria in porous media. PLoS One 16 (7 July). https://doi.org/10.1371/journal.pone.0254676.

Rajasekar, A., Zhao, C., Wu, S., Murava, R.T., Wilkinson, S., 2024. Synergistic biocementation: harnessing comamonas and bacillus ureolytic bacteria for enhanced sand stabilization. World J. Microbiol. Biotechnol. 40 (7), 1–15. https://doi.org/10.1007/S11274-024-04038-3/TABLES/5.

Rajasekar, A., Zhao, C., Wu, S., Murava, R.T., Norgbey, E., Omoregie, A.I., Moy, C.K.S., 2025. Removal of high concentrations of zinc, cadmium, and nickel heavy metals by bacillus and comamonas through microbially induced carbonate precipitation. Biodegradation 36 (3), 1–18. https://doi.org/10.1007/S10532-025-10131-7/FIGURES/11.

Satarug, S., Massányi, P., Caito, S., Davidova, S., Milushev, V., Satchanska, G., 2024. The mechanisms of cadmium toxicity in living organisms. Toxics 12 (12), 875. https://doi.org/10.3390/TOXICS12120875, 2024, Vol. 12, Page 875.

Schoofs, H., Schmit, J., Rink, L., 2024. Zinc toxicity: understanding the limits. Molecules 29 (13), 3130. https://doi.org/10.3390/MOLECULES29133130.

Shan, B., Hao, R., Xu, H., Li, J., Li, Y., Xu, X., Zhang, J., 2021. A review on mechanism of biomineralization using microbial-induced precipitation for immobilizing lead ions. Environ. Sci. Pollut. Control Ser. 28 (24), 30486–30498. https://doi.org/10.1007/S11356-021-14045-8, 2021 28:24.

Shi, Z., Qi, X., Zeng, X. an, Lu, Y., Zhou, J., Cui, K., Zhang, L., 2021. A newly isolated bacterium Comamonas sp. XL8 alleviates the toxicity of cadmium exposure in rice seedlings by accumulating cadmium. J. Hazard Mater. 403. https://doi.org/10.1016/j.jhazmat.2020.123824.

Singh, B., Christina, E., 2022. Indigenous microorganisms as an effective tool for in situ bioremediation. In: Relationship Between Microbes and the Environment for Sustainable Ecosystem Services, Volume 2: Microbial Mitigation of Waste for Sustainable Ecosystem Services, 5, pp. 273–295. https://doi.org/10.1016/B978-0-323-89937-6.00013-9.

Tyagi, M., da Fonseca, M.M.R., de Carvalho, C.C.C.R., 2011. Bioaugmentation and biostimulation strategies to improve the effectiveness of bioremediation processes. Biodegradation 22 (2), 231–241. https://doi.org/10.1007/S10532-010-9394-4.

Wang, L., Ji, B., Hu, Y., Liu, R., Sun, W., 2017. A review on in situ phytoremediation of mine tailings. Chemosphere 184, 594–600. https://doi.org/10.1016/j.chemosphere.2017.06.025.

Wang, Y., Wang, Y., Soga, K., DeJong, J.T., Kabla, A.J., 2023. Microscale investigations of temperature-dependent microbially induced carbonate precipitation (MICP) in the temperature range 4–50 °C. Acta Geotech. 18 (4), 2239–2261. https://doi.org/10.1007/s11440-022-01664-9.

Wang, G., Zhang, Z., Song, J., Luo, X., Tian, J., Xiao, Q., He, S., Liu, Y., 2025. Stable immobilization of uranium(VI) mediated by highly efficient indigenous microbes: dynamic behavior and mechanisms. J. Radioanal. Nucl. Chem. 334 (8), 5499–5511. https://doi.org/10.1007/S10967-025-10306-9/FIGURES/8.

Werner, T.T., Bell, C., Frenzel, M., Jowitt, S.M., Agarwal, P., Mmudd, G., 2024. Cadmium: a global assessment of mineral resources, extraction, and indicators of mine toxicity potential. Environ. Res. Lett. 19, 124091.

Wu, W., Ke, T., Zhou, X., Li, Q., Tao, Y., Zhang, Y., Zeng, Y., Cao, J., Chen, L., 2022. Synergistic remediation of copper mine tailing sand by microalgae and fungi. Appl. Soil Ecol. 175, 104453. https://doi.org/10.1016/j.apsoil.2022.104453.

Wu, C., Chen, Y., Qian, Z., Chen, H., Li, W., Li, Q., Xue, S., 2023. The effect of extracellular polymeric substances (EPS) of iron-oxidizing bacteria (Ochrobactrum EEELCW01) on mineral transformation and arsenic (As) fate. J. Environ. Sci. (China) 130, 187–196. https://doi.org/10.1016/J.JES.2022.10.004.

Xie, X., Fu, J., Wang, H., Liu, J., 2010. Heavy metal resistance by two bacteria strains isolated from a copper mine tailing in China. Afr. J. Biotechnol. 9 (26), 4056–4066. https://doi.org/10.5897/AJB2010.000-3286.

Xie, Y., He, N., Wei, M., Wen, T., Wang, X., Liu, H., Zhong, S., Xu, H., 2021. Cadmium biosorption and mechanism investigation using a novel Bacillus subtilis KC6 isolated from pyrite mine. J. Clean. Prod. 312, 127749. https://doi.org/10.1016/J.JCLEPRO.2021.127749.

Yin, Y., Han, J., Wu, H., Lu, Y., Bao, X., Lu, Z., 2024. *Comamonas resistens sp. Nov. and Pseudomonas triclosanedens sp. Nov.,* two members of the phylum Pseudomonadota isolated from the wastewater treatment system of a pharmaceutical factory. Int. J. Syst. Evol. Microbiol. 74 (1). https://doi.org/10.1099/IJSEM.0.006222.

Zeng, C., Hu, H., Feng, X., Wang, K., Zhang, Q., 2020. Activating CaCO3 to enhance lead removal from lead-zinc solution to serve as green technology for the purification of mine tailings. Chemosphere 249, 126227. https://doi.org/10.1016/j.chemosphere.2020.126227.

Zeng, Y., Chen, Z., Du, Y., Lyu, Q., Yang, Z., Liu, Y., Yan, Z., 2021. Microbiologically induced calcite precipitation technology for mineralizing lead and cadmium in landfill leachate. J. Environ. Manag. 296, 113199. https://doi.org/10.1016/J.JENVMAN.2021.113199.

Zhan, Q., Qian, C., 2016. Microbial-induced remediation of Zn2+ pollution based on the capture and utilization of carbon dioxide. Electron. J. Biotechnol. 19 (1), 29–32. https://doi.org/10.1016/j.ejbt.2015.11.003.

Zhang, W., Liu, Q., Manna, B., Singhal, N., Wang, J., Lyu, B., Zhou, X., Qian, Y., 2026. Metabolic rewiring and morphological adaptations drive bacterial strain-specific cadmium defense in the Yangtze river estuary. Microbiol. Res. 302. https://doi.org/10.1016/J.MICRES.2025.128326.

Zhou, Q., Yang, N., Li, Y., Ren, B., Ding, X., Bian, H., Yao, X., 2020. Total concentrations and sources of heavy metal pollution in global river and lake water bodies from 1972 to 2017. Glob. Ecol. Conserv. 22, e00925. https://doi.org/10.1016/J.GECCO.2020.E00925.

Zhuang, D., Yan, H., Tucker, M.E., Zhao, H., Han, Z., Zhao, Y., Sun, B., Li, D., Pan, J., Zhao, Y., Meng, R., Shan, G., Zhang, X., Tang, R., 2018. Calcite precipitation induced by Bacillus cereus MRR2 cultured at different Ca2+ concentrations: further insights into biotic and abiotic calcite. Chem. Geol. 500, 64–87. https://doi.org/10.1016/J.CHEMGEO.2018.09.018.

Zhuang, D., Yao, W., Guo, Y., Chen, Z., Gui, H., Zhao, Y., 2025. Bioremediation of heavy metal-contaminated solution and aged refuse by microbially induced calcium carbonate precipitation: further insights into Sporosarcina pasteurii. Microorganisms 13 (1), 64. https://doi.org/10.3390/MICROORGANISMS13010064/S1.